The current issue and full text archive of this journal is available at
www.emeraldinsight.com/0961-5539.htm

Heat transfer enhancement and pressure drop reduction due to mixed convection between two vertical parallel plates

Esmail M.A. Mokheimer, S. Sami and B.S. Yilbas
Mechanical Engineering Department, King Fahd University of Petroleum and Minerals, Dhahran, Saudi Arabia

Received 4 May 2009
Revised 4 September 2009
Accepted 20 October 2009

Abstract

Purpose – This paper's aim is to examine flow and heat transfer through vertical channels between parallel plates, which is of prime importance in the design of cooling systems for electronic equipment such as that of finned cold plates in general, plate-and-frame heat exchangers, etc.
Design/methodology/approach – Numerical and analytical solutions are presented to investigate the heat transfer enhancement and the pressure drop reduction due to buoyancy effects (for buoyancy-aided flow) for the developing laminar mixed convection in vertical channel between parallel plates in the vicinity of the critical values of the buoyancy parameter (Gr/Re)crt that are obtained analytically. The numerical solutions are presented for a wide range of the buoyancy parameters Gr/Re that cover both of buoyancy-opposed and buoyancy-aided flow situations under each of the isothermal boundary conditions under investigation.
Findings – Buoyancy parameters greater than the critical values result in building-up the pressure downstream of the entrance such that the vertical channel might act as a thermal diffuser with possible incipient flow reversal. Locations at which the pressure gradient vanishes and the locations at which the pressure-buildup starts have been numerically obtained and presented for all the investigated cases.
Research limitations/implications – The study is limited to the laminar flow situation.
Practical implications – The results clearly show that for buoyancy-aided flow, the increase of the buoyancy parameter enhances the heat transfer and reduces the pressure drop across the vertical channel. These findings are very useful for cooling channel or chimney designs.
Originality/value – The study is original and presents new findings, since none of the previous studies reported the conditions for which pressure buildup might take place due to mixed convection in vertical channels between parallel plates.
Keywords Flow, Heat transfer, Pressure, Plate structures
Paper type Research paper

Nomenclature

A, B	Integration constants of Equation (20)
C_1, C_2	Coefficients of Equation (21)
C_3	Coefficients of Equation (24) for forced flow
C_P	Specific heat of the fluid
b	Gap width between the parallel plates
D_h	Characteristic length of the vertical channel; b
dP/dZ	Dimensionless pressure gradient
F	Body force per unit volume, Equation (2)
Gr	Grashof number $g\beta(T_w - T_o)D_h^3/\upsilon^2 = g\beta(T_w - T_o)b^3/\upsilon^2$
Gr/Re	Buoyancy parameter

The authors gratefully acknowledge the support of King Fahd University of Petroleum and Minerals to carry out this work.

International Journal of Numerical Methods for Heat & Fluid Flow
Vol. 20 No. 8, 2010
pp. 867-896

0961-5539
DOI 10.1108/09615531011081414

$(Gr/Re)_{crt}$	Critical value of buoyancy parameter
p	Local pressure at any cross section of the vertical channel
p_o	Hydrostatic pressure, $\rho_o gz$ at channel entrance
P	Dimensionless pressure inside the channel at any cross section $(p - p_o/\rho u_o^2)$
Pr	Prandtl number $(\mu C_p/k)$
Q'''	Rate of heat generation per unit volume, Equation (3)
Re	Reynolds number $(\rho u_o D_h/\mu)$ $(= \rho u_o b/\mu)$
T_o	Ambient or fluid inlet temperature
T_w	Isothermal temperature of the heated wall
T_1, T_2	Isothermal temperatures of plate 1 and plate 2 of parallel plates
u	Axial velocity component
$\bar{u}$	Average axial velocity
u_o	Uniform entrance axial velocity
U	Dimensionless axial velocity at any point (u/u_o)
v	Transverse velocity component
V	Dimensionless transverse velocity $(v\,\mathrm{Re}/u_o)$
y	y-coordinate of the vertical channel between parallel plates
Y	Dimensionless y-coordinate (y/D_h)
z	Axial coordinate (measured from the channel entrance)
Z	Dimensionless axial coordinate in Cartesian coordinate systems $(z/D_h\mathrm{Re})$
Z_I	Distance from the channel entrance to the locations of zero pressure gradient
Z_{II}	Distance from the channel entrance to the locations of zero pressure
Z_{in}	Distance from the channel entrance to the location of numerical instability
Z_{fr}	Distance from the channel entrance to the location of onset of flow reversal
Z_{fd}	Distance from the channel entrance to the location of hydrodynamic fully development length

Greek letters

θ	Dimensionless temperature $(T - T_o)/(T_w - T_o)$
θ_T	Wall temperature difference ratio $(T_2 - T_o/T_1 - T_o)$
ρ	Density of the fluid
ρ_o	Density of the fluid at the channel entrance
μ	Dynamic viscosity of the fluid
υ	Kinematic viscosity of the fluid (μ/ρ)
β	Volumetric coefficient of thermal expansion

Subscripts

fd	Fully developed
forced	Forced flow
mxd	Mixed Convection
Crt	Critical

1. Introduction

The analysis of flow and heat transfer through vertical channels between parallel plates is of prime importance in the design of cooling systems for electronic equipment such as that of finned cold plates in general, plate-and-frame heat exchangers, etc. In

such systems, analysis of the combined free and forced convection in a channel provides information on the flow structure in the developing region and reveals the different length scales accompanying the different convective mechanisms operating in the developing flow region.

Even though most equipment is designed for operation in the turbulent flow regime, laminar flow has to be considered for partial load operation. Under these conditions, mixed convection through the vertical channels between parallel plates has been of interest in research for many years. The early research related to flow and heat transfer under mixed convection through parallel plate channels has been well cited by Inagaki and Komori (1995). Some of this early work includes studies by Cebeci *et al.* (1982) and Aung and Worku (1986a). Using dimensionless parameters, Aung and Worku (1986a) obtained a criterion for the existence of reversed flow under thermal boundary conditions of uniform heating on one wall while the other wall was thermally insulated. Yao (1983) studied mixed convection in vertical channel between parallel plates with symmetric uniform temperature and symmetric uniform flux heating and conjectured that fully developed flow might consist of periodic reversed flow. Barletta (2001) analytically investigated laminar and fully developed mixed convection in a vertical rectangular duct under thermal boundary conditions such that at least one of the four duct walls is kept isothermal. In this study, special attention was devoted to two sets of thermal boundary conditions:

(1) two facing duct walls were kept isothermal with different temperatures and the others are kept insulated; and

(2) two facing duct walls had a uniform wall heat flux and the others are kept isothermal with the same temperature.

In both cases, the conditions for the onset of flow reversal were obtained. Boulama and Galanis (2004) presented exact solutions for fully developed, steady state laminar mixed convection between parallel plates for thermal boundary conditions of uniform wall temperature (UWT) and uniform heat flux (UHF). Their results showed that the buoyancy effects significantly improve heat and momentum transfer rates near the heated walls of the channel. They (Boulama and Galanis, 2004) also analyzed the conditions for flow reversal. Analyzing the behavior of the flow with opposing buoyancy forces, Hamadah and Wirtz (1991) obtained values of Gr/Re beyond which flow reversal takes place. Quantitative information on the effect of buoyancy forces on temperature and velocity fields has been provided in a numerical study reported by Aung and Worku (1986b). These authors noted that buoyancy effects dramatically increase the hydrodynamic development distance. With asymmetric heating, the bulk temperature is a function of Gr/Re and the ratio of temperature difference between the walls, θ_T, and decreases as θ_T is reduced. Wirtz and McKinley (1985) conducted laboratory experiments on downward mixed convection between parallel plates where one plate heated the fluid (i.e. buoyancy-opposed flow situation). Ingham *et al.* (1988) numerically investigated the steady laminar combined convection flow under asymmetric constant wall temperature boundary conditions. They recorded reversed flow in the vicinity of the cold wall for combinations of the buoyancy parameter Gr/Re and θ_T. Their results showed that for a fixed value of θ_T, heat transfer is most efficient for Gr/Re large and negative (i.e. buoyancy-opposed flow). They also found that for a fixed value of Gr/Re heat transfer is most efficient when the entry temperature of the fluid is equal to the temperature of the cold wall. A laminar developing flow was observed in the absence of heating. Gau *et al.* (1992) experimentally studied

buoyancy-assisted convection flow and heat transfer in a heated vertical channel between two parallel plates for situations where the buoyancy parameter Gr/Re^2 is relatively large. One of the plates was uniformly heated while the other was kept insulated. A uniform flow was made to enter the channel from the bottom. The reversed flow, which occurs initially near the channel exit, was visualized for the case when Gr/Re^2 is greater than a threshold value. Huang *et al.* (1995) carried out experimental studies of the mixed convection flow and heat transfer in a vertical convergent channel. One of the side walls which was kept in the vertical position was heated uniformly, and the opposite wall which had a convergence angle of 3^o was insulated. The ratio of the height to the width at the inlet of the channel was 15. During the experiments, the Reynolds number ranged from 100 to 4,000 and the buoyancy parameter, Gr/Re^2, ranged from 0.3 to 907. Flow structure inside the channel was visualized with a heated smoke wire. The visualization experiments showed that for both assisted and opposed convection, flow reversal occurs only in the upstream of the channel but not in the downstream where rapid acceleration of flow occurs and the transport process is dominated by forced convection. Hammou *et al.* (2004) studied laminar mixed convection of humid air in a vertical channel with evaporation or condensation at the wall. The results showed that the effect of buoyancy forces on the latent Nusselt number is small. However, the axial velocity, the friction factor, the sensible Nusselt number and the Sherwood number are significantly influenced by buoyancy forces. Kasagi and Nishimura (1997) obtained direct numerical simulation for the fully developed combined forced and natural turbulent convection in a vertical plane channel between two parallel plates kept at different temperatures. Szpiro *et al.* (1984) presented numerical solutions for developing combined convection between uniformly heated vertical parallel plates

In a research pertinent to the buoyancy effects on the pressure development along a vertical channel, Han (1993), through his analysis of mixed convection in vertical pipes, proved that in buoyancy-aided flow situations with UHF, there is a certain point at which, the pressure gradient dP/dZ will become positive, i.e. the pressure will build up in the axial direction of the vertical heated pipe if the pipe is tall (long) enough. In this regard, Behzadmher *et al.* (2003) showed Re-Gr combinations that result in a pressure increase over the tube length from those resulting in a pressure decrease. They reported the values of Gr above which a pressure increase, rather than a pressure decrease, will take place over the tube length in the flow direction due to the buoyancy effects as $Gr = 4 \times 10^5$ for $Re = 1{,}000$ and $Gr = 3 \times 10^5$ for $Re = 1{,}500$. Recently, Mete and Orhan (2007) presented exact analytical results for fully developed mixed convective heat transfer of a Newtonian fluid in an open-ended vertical parallel plate microchannel with asymmetric wall heating at uniform heat fluxes. The velocity slip and the temperature jump at the wall are included in the formulation. The effects of the modified mixed convection parameter, Gr/Re, the Knudsen number, Kn and the ratio of wall heat flux, on the microchannel hydrodynamic and thermal behaviors are determined. Cimpean *et al.* (2009) considered a fully developed mixed convection flow between inclined parallel flat plates filled with a porous medium through which there is a constant flow rate and with heat being supplied to the fluid by the same uniform heat flux on each plate. They developed non-dimensional equations governing this flow that are seen to depend on two dimensionless parameters, a mixed convection parameter and the Péclet number, as well as the inclination of the plates to the horizontal.

The thorough literature cited above revealed that most of the work reported on mixed convection in vertical channels between parallel plates emphasized the

buoyancy effects on the heat transfer parameters (Inagaki and Komori, 1995; Cebeci *et al.*, 1982; Aung and Worku, 1986a; Yao, 1983; Barletta, 2001; Boulama and Galanis, 2004; Hamadah and Wirtz, 1991; Aung and Worku, 1986b; Wirtz and McKinley, 1985; Ingham *et al.*, 1988; Gau *et al.*, 1992; Huang *et al.*, 1995; Hammou *et al.*, 2004; Kasagi and Nishimura, 1997; Szpiro *et al.*, 1984; Mete and Orhan, 2007; Cimpean *et al.*, 2009). Some of this work gave attention to the flow reversal phenomena for buoyancy-opposed flow situations (i.e. for upward flow in a cooled channel or downward flow in a heated channel; Aung and Worku, 1986a; Yao, 1983; Barletta, 2001; Boulama and Galanis, 2004; Hamadah and Wirtz, 1991; Aung and Worku, 1986b; Wirtz and McKinley, 1985; Ingham *et al.*, 1988). None of this previous work investigated or justified the presence of flow reversal for buoyancy-aided flow situations. On the other hand, available in the literature are a limited number of research articles that emphasized the buoyancy effects on the hydrodynamic flow parameters of mixed convection in vertical channels between parallel plates such as the pressure gradient and pressure drop (Han, 1993; Behazadmher *et al.*, 2003). The literature analysis revealed also that the pressure buildup through a vertical channel due to mixed convection was implicitly shown by Aung and Worku (1986b), El-Shaarawi and Sarhan (1980) and Mokheimer and El-Sharawi (2004a). This pressure buildup might be the cause of flow reversal in buoyancy-aided flow situations. Mokheimer and El-Sharawi (2004b) demonstrated and proved the presence of critical values of Gr/Re at which the pressure gradient vanishes and beyond which pressure buildup takes place due to mixed convection in vertical eccentric annuli under thermal boundary conditions of third kind. Recently, the present authors, Mokheimer and Sami (2006), obtained and presented the critical values of Gr/Re for mixed convection in vertical eccentric annuli under thermal boundary conditions of first kind. However, none of the previous studies reported the conditions for which pressure buildup might take place due to mixed convection in vertical channels between parallel plates. In other words, none of the previous work exactly reported the values of the buoyancy parameters Gr/Re for which the pressure gradient becomes zero and above which positive pressure gradient might prevail along vertical channels between parallel plates leading to a pressure buildup rather than pressure drop downstream the entrance of such vertical channels under mixed convection conditions. Moreover, none of the previous studies reported exactly the locations at which pressure gradient starts to be positive and/or the positions at which the pressure buildup commences in a vertical channel between parallel plates due to buoyancy effects. The importance of the careful analysis, the lack of exact information regarding the hydrodynamic behavior of laminar flow under mixed convection conditions motivated the authors to investigate the laminar mixed convection in vertical channels, in general (Sami, 2005).

The first objective of the present study is to present the critical values of Gr/Re for which the pressure gradient (dP/dZ) becomes zero for fully developed mixed convection in vertical channels between parallel plates under isothermal boundary conditions. In this regard, the exact values of these critical values of the buoyancy parameters are to be presented for the first time in the public literature.

The second objective of the present study is to numerically investigate the heat transfer enhancement and the pressure drop reduction due to buoyancy effects (for buoyancy-aided flow) for the developing laminar mixed convection in vertical channel between parallel plates in the vicinity of the critical values of the buoyancy parameter $(Gr/Re)_{crt}$ that are obtained analytically. The numerical solutions are presented for a wide range of the buoyancy parameters Gr/Re that cover both of buoyancy-opposed and buoyancy-aided flow situations under each of the isothermal boundary conditions

under investigation. Numerical solutions for buoyancy-aide flow situations with $Gr/Re > (Gr/Re)_{crt}$ are used to calculate and present for the first time the exact locations at which pressure gradient starts to be positive and/or the positions at which the pressure buildup commences in a vertical channel between parallel plates. The buoyancy effects on changing these locations downstream the channel entrance are investigated over a wide range of the buoyancy parameter Gr/Re. The effect of Prandtl number on the hydrodynamic behavior of the mixed convection flow is also targeted in this study. Moreover, the heat transfer enhancement presented by the amount the heat absorbed by the fluid from the channel walls per unit of the pumping power is obtained and presented for the first time.

2. Problem formulation and governing equations

The general governing equations of flow and heat transfer are the conservation equations of mass, momentum (Navier-Stokes equations) and energy. Assuming constant physical properties, one can write the full conservation equations in a vectorial form as follows.

Continuity equation

$$\nabla . V = 0 \tag{1}$$

Momentum equation

$$\rho \frac{DV}{Dt} = F - \nabla P + \mu \nabla^2 V \tag{2}$$

Energy equation

$$\rho C_p \frac{DT}{Dt} = k \nabla^2 T + Q''' + \mu \, \Phi \tag{3}$$

It is worth mentioning that the left-hand side of Equation (2) represents the inertia forces; the terms on the right-hand side denote the body force (buoyancy), the pressure gradient that represents the external driving forces (that are provided via a pump, a fan, a blower, a compressor, a valve, etc.), and viscous friction forces, respectively. The superimposition of forced convection and natural convection and the interaction between their driving forces in mixed convection flows is well explained by Han (1993).

For the problem under consideration, Figure 1 depicts two-dimensional channel between two vertical parallel plates. The distance between the plates is "b" i.e. the channel width. The Cartesian coordinate system is chosen such that the positive z-axis is in the vertical direction and points to the flow direction. The gravitational body force per unit mass "g" is always acting downwards. The y-axis is orthogonal to the channel walls, and the origin of the axes is such that the positions of the channel walls are at $y = 0$ and $y = b$.

The flow is assumed to be steady with negligible viscous dissipation and internal heat generation. The body forces other than the gravitational body force are absent everywhere. The fluid is assumed to be a Newtonian fluid of constant properties but obeys the Boussinesq approximation. Thus, the density of the fluid will vary only in the gravitational body force term as function of the temperature according to Boussinesq approximation. Assuming that the depth of the channel is very large compared to its width and height, two-dimensional flow conditions can be considered.

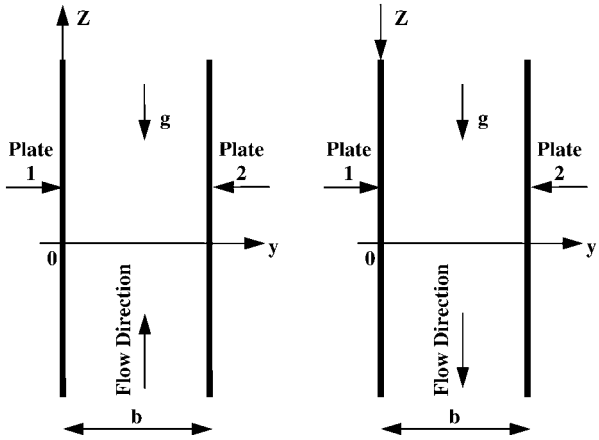

Figure 1.
Schematic view of the system and coordinate axes corresponding to (a) upflow and (b) downflow

The flow is assumed to be hydrodynamically as well as thermally developing through the vertical channel between the two parallel plates. In the present study, uniform flow temperature (T_o) and uniform flow velocity (u_o) were assumed at the channel entrance. The boundary layer approximation along with the uniform inlet velocity and temperatures is adopted in line with the previous studies (Aung and Worku, 1986b; Han, 1993; El-Shaarawi and Sarhan, 1980; Du *et al.*, 1998; Barletta *et al.*, 2006). Moreover, the justification of the boundary layer approximation and uniform inlet conditions for mixed convection in the entrance region of vertical channels can be found in the previous studies (Aung, 1987).

After performing order of magnitude analysis that is based on the boundary layer approximation, the momentum equation in the transverse direction reduces to $-\partial p/\partial y = 0$, which implies that the pressure along the channel does not vary in the transverse direction and varies only in the vertical (axial) flow direction, applying the Boussinesq approximation and using the pertinent dimensionless parameters given in the nomenclature, the governing equations can be written in dimensionless form as:

Continuity equation

$$\frac{\partial U}{\partial Z} + \frac{\partial V}{\partial Y} = 0 \tag{4}$$

Z-momentum equation

$$\left[U\frac{\partial U}{\partial Z} + V\frac{\partial U}{\partial Y}\right] = -\frac{\partial P}{\partial Z} \pm \frac{Gr}{\mathrm{Re}}\theta + \left(\frac{\partial^2 U}{\partial Y^2}\right) \tag{5}$$

where the $+$ and $-$ signs of the ($\pm$) sign of the buoyancy term in the above equation are for *buoyancy-aided flow* and *buoyancy-opposed flow*, respectively.

Energy equation

$$U\frac{\partial \theta}{\partial Z} + V\frac{\partial \theta}{\partial Y} = \frac{1}{\mathrm{Pr}}\left(\frac{\partial^2 \theta}{\partial Y^2}\right) \tag{6}$$

Equations (4)-(6) are subjected to the following boundary conditions:

$$\begin{aligned} &\text{At } Z = 0, \quad 0 < Y < 1: \; U = 1, \quad V = P = \theta = 0 \\ &Z > 0, \quad Y = 0: \; U = V = 0, \quad \theta = 1 \\ &Z > 0, \quad Y = 1: \; U = V = 0, \quad \theta = \theta_T \end{aligned} \tag{7}$$

It is worth noting here that the entering fluid temperature has been used as a reference temperature in the Boussinesq approximation and the expression for the dimensionless temperature for the two cases of fully developed and developing flow. In spite of being bizarre for the fully developed flow problem modeling, the use of the entering fluid temperature as a reference was deliberately adopted for the sake of comparison between the analytical solution obtained for the fully developed flow and that obtained numerically from the numerical solution of the developing problem at great distances from the entrance. It is worth mentioning here also that the entering fluid temperature has been used as the reference temperature by Aung and Worku (1986a, b) and Hamadah and Writze (1991) in their analysis of mixed convection in vertical channels between parallel plates. On the other hand, Barletta and Zanchini (1999) set the reference temperature equal to the arithmetic mean temperature over the cross section of the duct while Boulama and Galanis (2004) adopted the temperature of the cooler wall as reference due to its physical convenience and simplicity in expressing the thermal boundary conditions. This is consistent with our choice of the reference temperature for the case of $\theta_T = 0$. It is worth noting here that P in the momentum equation is the pressure difference between the local pressure at any location (height) of the channel and the pressure at the channel inlet. Thus, at the channel inlet P in Equation (7) will be zero.

3. General analysis and fully developed analytical solutions

The analytical solutions of the governing equations in the fully developed region are derived here in order to demonstrate the presence of critical values of the buoyancy parameter Gr/Re at which the pressure gradient $(dP/dZ)_{fd}$ vanishes and above which pressure builds up in the flow direction in vertical channels due to the buoyancy effects. Moreover, the analytical solutions obtained will be used to determine the critical values of Gr/Re.

The assumption of a fully developed mixed convection flow implies, here, that the flow is both hydrodynamically and thermally fully developed. Under such conditions, the transverse velocity component vanishes and the axial velocity component becomes invariant in the flow direction, i.e. $(\partial U/\partial Z) = 0$. Moreover, heating (or cooling) with at least one of the walls is kept isothermal, makes $(\partial\theta/\partial Z) = 0$ in the fully developed region. Thus, the governing equations pertinent to the problem of fully developed laminar mixed convection between vertical parallel plates for both buoyancy-aided and buoyancy-opposed flows are written as:

$$\left(-\frac{dP}{dZ}\right)_{fd,\,mxd} \pm \frac{Gr}{\mathrm{Re}}\theta + \left(\frac{d^2U}{dY^2}\right) = 0 \tag{8}$$

$$\frac{d^2\theta}{dY^2} = 0 \tag{9}$$

It is worth mentioning here that under the fully developed conditions U and θ are

functions of Y only while the pressure is not a function of Y. Thus, the pressure gradient *(dP/dZ)* is constant to satisfy Equation (8). On the other hand, the general solution for the fully developed energy equation (9) can be obtained by integrating Equation (9) twice and its general form can be written as:

$$\theta = AY + B \tag{10}$$

where A and B are the integration constants that are to be evaluated under the isothermal boundary conditions given in Equation (7) and are given as: $A = \theta_T - 1, B = 1$.

Substituting Equation (10) into Equation (8), one can write the axial momentum equation as:

$$\frac{d^2U}{dY^2} + C_1 Y + C_2 = 0 \tag{11}$$

where

$$C_1 = \pm\frac{Gr}{\mathrm{Re}}A \quad \text{and} \quad C_2 = \left(-\frac{dP}{dZ}\right)_{fd,\,mxd} + \left(\pm\frac{Gr}{\mathrm{Re}}\right)B.$$

Integrating Equation (11) twice and applying the no slip boundary conditions ($U = 0$) at both walls (i.e. at $Y = 0$ and $Y = 1$), one can obtain the general solution for the axial velocity ($U_{fd,\,mxd}$) as:

$$U_{fd,mxd} = \left(\left(-\frac{dP}{dZ}\right)_{fd,\,mxd} + \left(\pm\frac{Gr}{\mathrm{Re}}\right)B\right)\frac{Y(1-Y)}{2} + \left(\pm\frac{Gr}{\mathrm{Re}}\right)A\frac{Y(1-Y^2)}{6} \tag{12}$$

or simply:

$$U_{fd,\,mxd} = C_2\frac{Y(1-Y)}{2} + C_1\frac{Y(1-Y^2)}{6} \quad \text{where } C_1 \text{ and } C_2 \text{ are as defined above.} \tag{13}$$

It is worth noting here that the fully developed velocity profile for pure forced flow can be obtained from Equation (12) by just equating the buoyancy-force term to zero, i.e. putting Gr/Re = 0 in Equation (12). Thus the velocity profile for pure forced flow is:

$$U_{fd,forced} = C_3\frac{Y(1-Y)}{2} \quad \text{where } C_3 = \left(-\frac{dP}{dZ}\right)_{fd,forced} \tag{14}$$

3.1 Calculation of critical value of the buoyancy parameter $(Gr/Re)_{crt}$ for isothermal boundary conditions

The average axial velocity at any section of the channel is the same for both forced and mixed convection which is equal to 1. This is because of steady flow satisfaction. Thus, one can write:

$$u_{average}/u_o = \bar{U}_{fd,forced} = \bar{U}_{fd,mxd} = 1$$

Therefore, the integral form of continuity equation for both forced convection and mixed convection can be written as:

$$\int_0^1 U_{fd,forced} dY = \int_0^1 U_{fd,mxd} dY \tag{15}$$

Substituting the velocity profile for the mixed convection flow given by Equation (13) and for that of the pure forced flow given by Equation (14) into Equation (15), one gets:

$$\int_0^1 C_3 \frac{Y(1-Y)}{2}\, dY = \int_0^1 \left[C_2 \frac{Y(1-Y)}{2} + C_1 \frac{Y(1-Y^2)}{6} \right] dY$$

After integrating, one gets:

$$\left(\frac{dP}{dZ}\right)_{fd,mxd} = \left(\frac{dP}{dZ}\right)_{fd,forced} + \left(\pm \frac{Gr}{\mathrm{Re}}\right)\left(\frac{A}{2} + B\right) \tag{16}$$

where $(dP/dZ)_{fd,forced}$ is the pressure gradient due to pure forced flow and can be obtained via applying the integral form of the continuity equation for pure forced flow as follows:

$$\int_0^1 U_{fd,forced} dY = 1$$

Substituting for the velocity profile for pure forced flow given by Equation (14) into the above equation, one gets:

$$\left(\frac{dP}{dZ}\right)_{fd,forced} = -12$$

Inspecting Equation (16), one should keep in mind the following facts. For pure forced flow, the pressure gradient $(dP/dZ)_{fd,forced}$ is always of negative value as derived above. On the other hand, the value of the constant A ranges between -1 and 0 for the isothermal boundary conditions under considerations including all the values of θ_T, ($\theta_T = 0$ to 1), and it will be always positive for any value of θ_T >1. Moreover, the constant B in Equation (16) is always positive and equals to 1 for the isothermal boundary conditions considered. Thus the value of the quantity $(A/2) + B$ is always positive, i.e. $((A/2) + B) \geq 0$. Thus, it can be clearly seen from the above equation, Equation (26), and the above discussion that the pressure gradient $(dP/dZ)_{fd,mxd}$ might vanish if and only if the buoyancy parameter term has the positive sign. This is possible only for the situations of buoyancy-aided flow. Thus, a general expression for the critical value of the buoyancy parameter, $(\mathrm{Gr/Re})_{\mathrm{crt}}$ at which the pressure gradient

becomes zero can be obtained by simply equating the pressure gradient due to mixed convection $(dP/dZ)_{fd,\ mxd}$, given by Equation (16), to zero which yields:

$$\left(\frac{Gr}{\mathrm{Re}}\right)_{crt} = \frac{2\left(-\frac{dP}{dZ}\right)_{fd,forced}}{(A+2B)} = \frac{2\left(-\frac{dP}{dZ}\right)_{fd,forced}}{(\theta_T+1)} = \frac{24}{(\theta_T+1)} \tag{17}$$

Equation (17) represents a general expression for the critical buoyancy parameter $(\mathrm{Gr/Re})_{\mathrm{crt}}$ at which the pressure gradient vanishes and above which the onset of pressure build-up takes place. Moreover, Equation (17) makes it possible to obtain the critical values of the buoyancy parameter, $(\mathrm{Gr/Re})_{\mathrm{crt}}$, under isothermal boundary conditions under consideration for any value of temperature ratio of the two isothermal walls, θ_T, via substituting the values of θ_T in Equation (17). Figure 2, given below, presents the critical values of buoyancy parameter $(\mathrm{Gr/Re})_{\mathrm{crt}}$ for different values of θ_T.

It is worth mentioning here that Equation (16) can be also used to evaluate analytically the fully developed pressure gradient for mixed convection flow in a vertical channel between parallel plates under isothermal boundary conditions, with different values of θ_T, over a wide range of the buoyancy parameter, Gr/Re, that covers buoyancy-opposed and buoyancy-aided mixed convection flows including the pure forced convection flow. These values are shown in Figure 3 for some of the investigated cases. It should be noted that the buoyancy parameter Gr/Re always takes a positive value according to its definition. However, the positive and negative signs used in front of the values of the buoyancy parameter in Figure 3 are due to the sign of the buoyancy term in the momentum equation, Equation (5), where the positive sign is used for buoyancy-aided flow situations while the negative sign is used for buoyancy-opposed flow situations as indicated earlier. It is quite clear from Figure 3 that buoyancy-opposed flow situations, the increase of the buoyancy increases the pressure drop across the channel

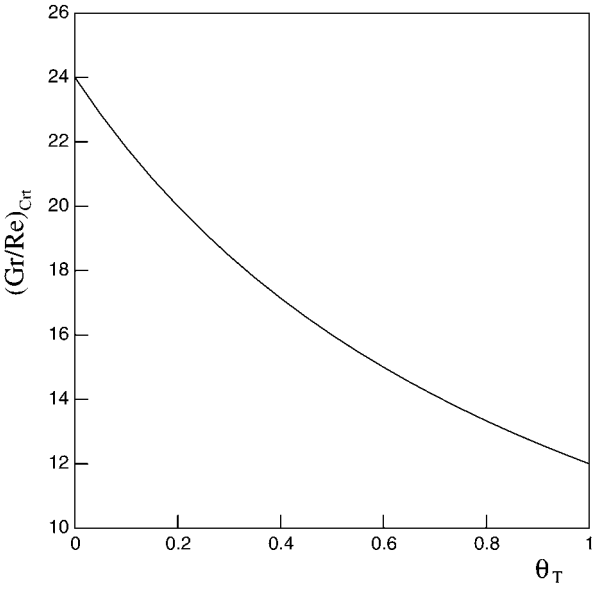

Figure 2.
Critical values of the buoyancy parameter Gr/Re for different values of θ_T

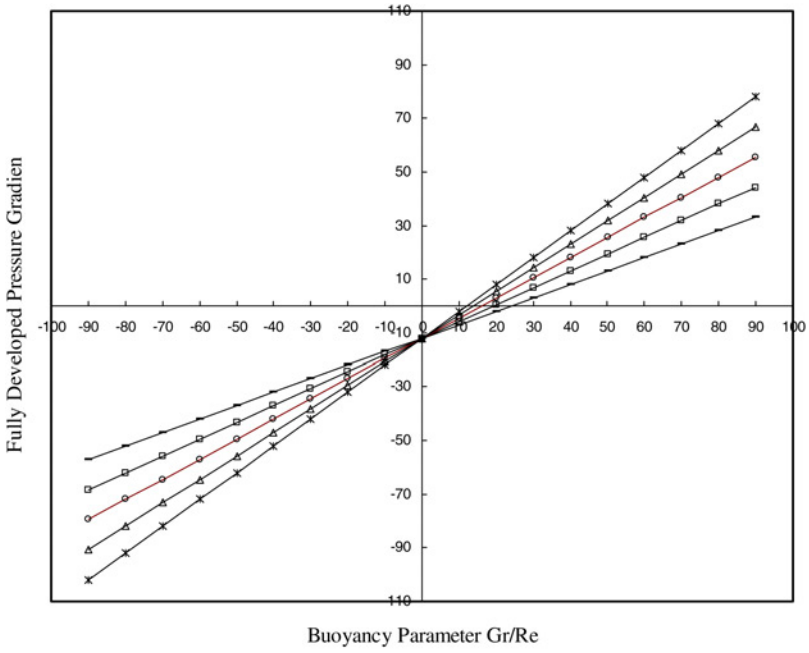

Notes: $\theta_T = 0$; □: $\theta_T = 0.25$; ○: $\theta_T = 0.5$; △: $\theta_T = 0.75$; ∗: $\theta_T = 1$

Figure 3.
Variation of the fully developed pressure gradient with the buoyancy parameter for different values of the walls temperature ratio

compared with the forced flow situations. However, for buoyancy-aided flow situations the fully developed pressure drop decreases with the increase of the buoyancy parameter. Moreover, the more increase of the buoyancy effects might lead to pressure build up. The values of the buoyancy parameter at which the pressure builds up for buoyancy-aided flow are those obtained analytically and given in Equation (17). The effect of the buoyancy on the pressure drop reduction and the heat transfer enhancement of the developing buoyancy-aided flow are presented in section 7 hereinafter.

3.2 Conditions for flow reversal under isothermal conditions

The fully developed velocity profile can be obtained via the back substitution of Equation (16) into Equation (12) and the obtained expression can be written as

$$U_{fd,mxd} = -6Y(Y-1) + \frac{1}{12}\left(\pm\frac{Gr}{\mathrm{Re}}\right)(1-\theta_T)(2Y^3 - 3Y^2 + Y) \qquad (18)$$

Equation (18) can be used to obtain an analytical expression for the condition (value of the buoyancy parameter (Gr/Re)) at which flow reversal commences in vertical channel between parallel plates under the isothermal boundary conditions. Flow reversal takes place when the velocity gradient in the transverse direction becomes less than or equal to zero; $(dU/dY) \leq 0$. This condition is usually encountered at the walls where the flow suffers the highest retarding resistance due to the viscous effects. Thus, the analytical expression for the condition of flow reversal is obtained via differentiating the velocity profile with respect to the transverse direction, Y, and applying the condition of flow reversal, $(dU/dY) \leq 0$. In applying this condition at the two walls,

one should take care of the positive direction of the Y-coordinate and the behavior of the velocity profile at the two walls. In this regard, one should notice that in case of flow reversal at the wall of $Y = 0$, the gradient is negative since the velocity changes from zero at the wall (no-slip conditions) to a negative value in the layer adjacent to the wall. On the other hand, in the case of flow reversal at the other wall of $Y = 1$, the velocity gradient acquires appositive gradient in the positive Y-direction such that it changes the velocity from a negative value (reversed flow) in the layer adjacent to the wall into a zero value at the wall (no-slip conditions). Thus, expressing the first derivative of the velocity profile with respect the transverse coordinate Y in the positive direction should be as per the following expressions:

$$\left.\frac{dU}{dY}\right|_{Y=0} \leq 0 \quad \text{and} \quad \left.\frac{dU}{dY}\right|_{Y=1} \geq 0 \tag{19}$$

Applying the above conditions for buoyancy-aided and buoyancy-opposed flows revealed that the values of the buoyancy parameter (Gr/Re) that makes flow reversal commence at one of the channel walls is given as:

$$\left(\frac{Gr}{\mathrm{Re}}\right) \geq \frac{72}{(1-\theta_T)} \tag{20}$$

The flow reversal would take place at the buoyancy-driving wall (the wall of $\theta_{\mathrm{T}} = 1$) for buoyancy-opposed flow situations and on the corresponding wall (the wall of $0 \leq \theta_{\mathrm{T}} < 1$) for buoyancy-aided flow situations. Figure 4, below, depicts the velocity

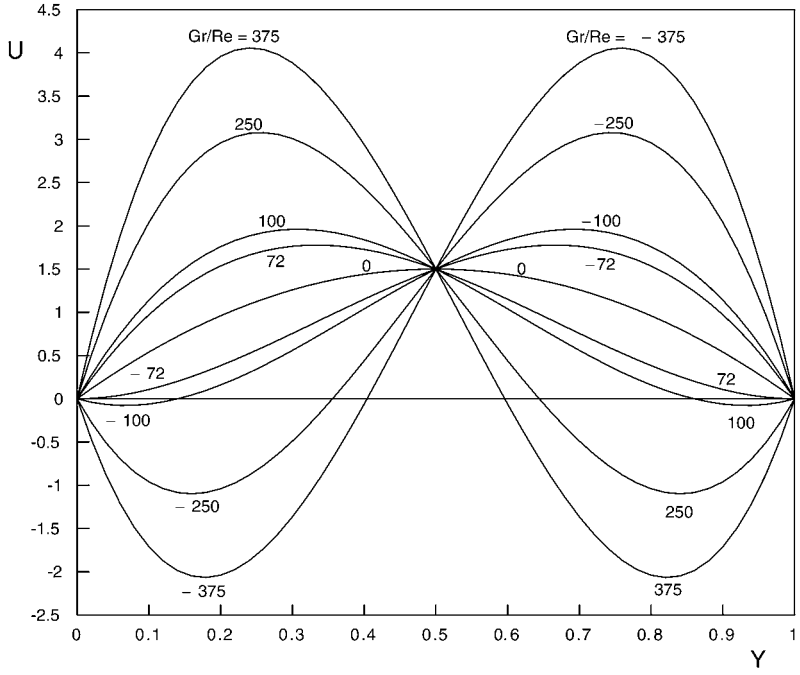

Figure 4.
Velocity profiles for the case of $\theta_{\mathrm{T}} = 0$, for buoyancy-aided and buoyancy-opposed flow situations of different values of Gr/Re

profiles for the case of $\theta_T = 0$ for different values of the buoyancy parameter Gr/Re for both buoyancy-aided and buoyancy-opposed flows as well as for pure forced flow, (Gr/Re) = 0. It is worth reminding here that the − signs in front of the buoyancy parameter in the label of some of velocity profiles in this graph stand for buoyancy-opposed flow while the positive numbers represent the buoyancy-aided flow as per the notations followed in this article. The velocity profiles clearly confirm the above discussion. It is quite clear that the flow reversal would commence for both situations of buoyancy-aided and buoyancy-opposed flows for the same value of the buoyancy parameter (i.e. (Gr/Re) = 72 for the case of $\theta_T = 0$) where the gradient of the velocity profiles is exactly zero for the two cases but at the opposite walls as discussed above and as clearly shown in Figure 4. For buoyancy parameters (Gr/Re) > 72 (for the case of $\theta_T = 0$) flow reversal takes place for both situations of buoyancy-aided and buoyancy-opposed flow but at the opposite walls. This result confirms that concluded by Barletta and Zanchini (1999). Moreover, the results presented in Figure 4 for buoyancy-opposed flow are identical to those presented by Boulama and Galanis (2004) with the notice that the values of the buoyancy parameters reported by Boulama and Galanis (2004) and Barletta and Zanchini (1999) are four and eight times the corresponding values reported in the present article, respectively. These differences among these particular three articles (Boulama and Galanis, 2004; Barletta and Zanchini, 1999 and present) are due to the three different definitions of the characteristic length used in defining the Grashof and Reynolds number. In the present work, the characteristic length was selected as the width of the channel in order to compare the present results with that of Aung and Worku (1986a, b) (particularly the numerical results of the developing region; Aung and Worku, 1986b). On the other hand, Boulama and Galanis (2004) defined the characteristic length as twice the channel width while Barletta and Zanchini (1999) defined it as four times half of the channel width. Thus, the criterion of flow reversal that is exactly the same for the three articles, was reported differently in the three article for the case of $\theta_T = 0$ as: (Gr/Re) $\geq$ 72 in the present work), (Gr/Re) $\geq$ 288 by Boulama and Galanis, 2004) and (Gr/Re) $\geq$ 576 by Barletta and Zanchini, 1999). It is worth reporting here that the work reported by Boulama and Galanis (2004) indicates that they studied the case of buoyancy-opposed flow for upward cooled flow. They did not report results for buoyancy-aided flow. On the other hand, Barletta and Zanchini (1999) reported that flow reversal will take place for both buoyancy-aided and buoyancy-opposed flow situations but at opposite walls if the buoyancy parameter exceeded specific limit. This conclusion is consistent with the findings of the present work as discussed above. The velocity profiles, shown in Figure 4, indicate that the velocity at the middle of the channel is independent of the buoyancy parameter Gr/Re. This is consistent with the findings of other researchers (Boulama and Galanis, 2004; Barletta and Zanchini, 1999).

4. Numerical scheme and method of solution

The flow and heat transfer governing equations in the developing region, Equations (4)-(6), subjected to the entrance conditions and the thermal and hydrodynamic boundary conditions, Equation (7) is solved numerically using standard finite difference techniques. In this regard, the dimensionless continuity equation, Equation (4) is written in the following finite difference form, according to Miyatake and Fujii (1972):

$$V(k) = \left\{ V(k-1) - \frac{\Delta Y}{2\Delta Z}\left[U(k-1) + U(k) - U^*(K-1) - U^*(k)\right] \right\}(1-Y) + \left\{ V^*(k+1) + \frac{\Delta Y}{2\Delta Z}\left[U(k+1) + U(k) - U^*(K+1) - U^*(k)\right] \right\}(Y) \tag{21}$$

The finite difference form of the dimensionless momentum equation, Equation (5) is:

$$U^*(k)\left[\frac{U(k) - U^*(k)}{\Delta Z}\right] + V^*(k)\left[\frac{U(k+1) - U(k-1)}{2\Delta Y}\right] = -\left[\frac{P(k) - P^*(k)}{\Delta Z}\right] + \left(\frac{Gr}{Re}\right)\theta(k) + \left[\frac{U(k+1) - 2U(k) + U(k-1)}{(\Delta Y)^2}\right] \tag{22}$$

The finite difference formulation of energy equation is:

$$U^*(k)\frac{\theta(k) - \theta^*(k)}{\Delta Z} + V^*(k)\left[\frac{\theta(k+1) - \theta(k-1)}{2\Delta Y}\right] = \frac{1}{\mathrm{Pr}}\left[\frac{\theta(k+1) - \theta(k-1) - 2\theta(k)}{(\Delta Y)^2}\right] \tag{23}$$

The superscript, *, in the above equations represents the previous axial step value. The integral continuity equation can be represented by employing a trapezoidal rule of numerical integration taking into consideration the no-slip conditions at the walls as follows:

$$\left[\sum_{k=2}^{n} U(k)\right]\Delta Y = 1 \tag{24}$$

5. Numerical results accuracy and code validation

5.1 Numerical results grid-independence tests

The numerical scheme developed above was tested for grid-independent solutions in the axial and transverse directions. In this regard, grids of mesh size of 10^{-5}, 10^{-7} and 10^{-10} were taken in the axial (flow), Z-direction near the entrance where the gradients are so high. This very small grid size in the Z-direction was gradually increased till it reaches a constant value of 10^{-3} near the fully developed region where the gradients of the flow and heat transfer parameters vanish. The preliminary results revealed that axial step starting with a value of 10^{-10} at the channel entrance and increases gradually in an exponential form till it reaches the value of 10^{-3} far downstream is the best to capture the high gradients and simulates the flow dynamics with the best accuracy near the entrance. Thus, all the results of the presented work were developed using the very fine grid size, of 10^{-10} in Z-direction near the entrance of the channel. On the other hand, different grid sizes were tested in the transverse Y-direction till numerical grid-independent results were obtained. The numerical value of the hydrodynamic fully development length, Z_{fd}, was taken as the criterion for the grid size independence test in the Y-direction. The fully developed length was defined in the present work as the length at which the developing

velocity profile approaches its pertinent fully developed analytical profile within 0.1 percent deviation. In this regard, Figure 5 summarizes the results of the grid independence test that was conducted at the beginning of the present work. It was observed that for coarse grid, the value of hydrodynamic fully development length is high and as the number of nodes increases in the Y-direction, the hydrodynamic fully development length decreases. No more significant variation in the value of fully developed length was recorded for the grid points or nodes greater than 50. This was also confirmed for other parameters such as the Nusselt number, the mean bulk fluid temperature, etc. Thus a numerical mesh of 50 grid points in the Y-direction was used to obtain all the results.

5.2 Numerical results accuracy

The numerical scheme and the developed solution code were validated by comparing the results obtained via the presently developed code with the pertinent results that are available in the literature. In this regard, special runs of the code were conducted for the pure forced flow, $Gr/Re = 0$. The presently obtained results via these special runs were compared with the results reported by Shah and London (1978). The results of such comparison revealed the values of the Nusselt number obtained via the present code far downstream the channel entrance are 4.0047 and 3.9951 on the heated and the cooled walls, respectively. These are corresponding to the value of 4 as reported by Shah and London (1978) with a maximum deviation of about 0.12 percent which represents an excellent agreement. Finally, the present numerical code was also validated via comparing the developing velocity profiles, pressure and mean bulk fluid temperature with that reported by Aung and Worku (1986b). The graphical comparisons presented in Figure 6 reveal an excellent agreement between the presently obtained results and that reported earlier by Aung and Worku (1986b). It is worth reporting here that velocity profiles far down stream the channel entrance obtained via all the computer runs of the numerical codes approached the pertinent fully developed analytically obtained velocity profiles within 0.1 percent deviation for all the values of the buoyancy parameter, Gr/Re including the situations of flow reversal that does not create flow and numerical instability. It is worth mentioning here that it would be better to validate the numerically obtained results against the pertinent experimental results, if available. However, there were no experimental results available for mixed convection in vertical channels between parallel plates under isothermal boundary conditions. The only experimental results available in the literature are those published

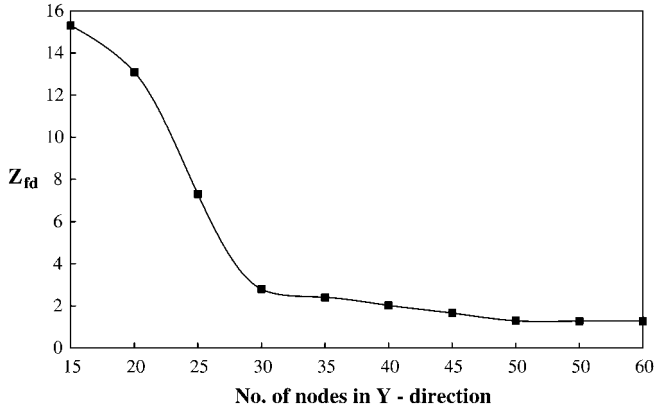

Figure 5.
Graphical representation of grid independence test

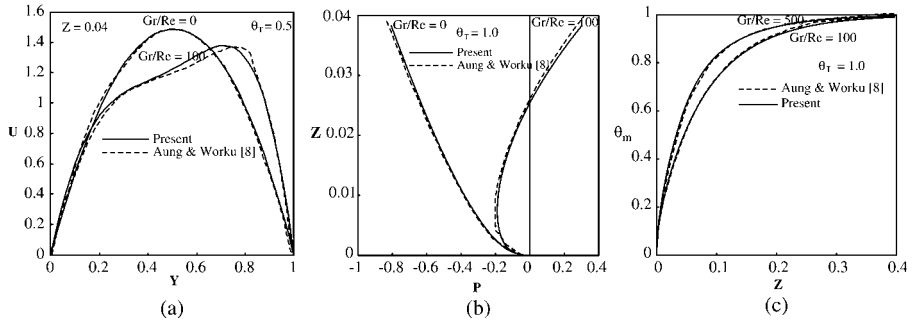

Notes: (a) Velocity profiles between present results and for (Gr/Re) = 0 and 100, $\theta_T = 0.5$ at dimensionless channel height Z = 0.04; (b) pressure variation (Gr/Re) = 0 and 100, $\theta_T = 1.0$ along the channel height (Z); (c) mean temperature (Gr/Re) = 100 and 500, $\theta_T = 1.0$ along the channel height (Z)

Figure 6.
Comparison between the present work and that of Aung and Worku (1986b)

in Gau *et al.* (1992) and Huang *et al.* (1995) for uniform heat flux and adiabatic walls. On the other hand, validation of the numerically obtained results with the pertinent analytical solutions, if available, against analytical solutions would represent a reasonable enough validation. In this regard, the critical values of the buoyancy parameter $(Gr/Re)_{crt}$ that were obtained analytically for the investigated thermal boundary conditions were used as input to the present numerical code and the pressure gradient in all the cases developed from its very high negative value at the entrance and asymptotically reached its exact value of the zero in the fully developed region. The development of the pressure gradient for these particular cases of $Gr/Re = (Gr/Re)_{crt}$ are plotted as dotted lines in Figures 7(a, c). Approaching the fully developed analytically obtained values for different parameters, exactly or within a negligible deviation, via the numerical code that solves the governing equations of the developing region far down the channel entrance represent an excellent validation of the developing region model, the numerical scheme and the presently developed computer code.

6. Numerical results presentation and discussion

Having the confidence in the mathematical model, numerical scheme and the computer code, the authors used the presently developed computer code to generate a huge amount of data for mixed convection in vertical channels between parallel plates under isothermal boundary conditions over a wide range of the buoyancy parameter Gr/Re. However, more emphasis was devoted to the buoyancy-aided flow situations. This was based on the fact that the pressure buildup takes place downstream a vertical channel only under buoyancy-aided flow conditions as discussed above and as reported earlier by Aung and Worku (1986b), Han (1993), Behazadmher *et al.* (2003), El-Shaarawi and Sarhan (1980), Mete and Orhan (2007), Cimpean *et al.* (2009), Mokheimer and El-Shaarawi (2004a, b), Mokheimer and Sami (2006) and Sami (2005).

Figures 7(a, b) depict the developments of the pressure gradient (dP/dZ) and the pressure defect (P), respectively, through the entrance region of a vertical channel between parallel plates under isothermal boundary conditions with $\theta_T = 0$ over a wide range of the buoyancy parameter Gr/Re. These two Figures 7(a, b) show that the dimensionless pressure defect develops from zero at the channel entrance with a very high negative pressure gradient at the entrance acquiring negative values due to the

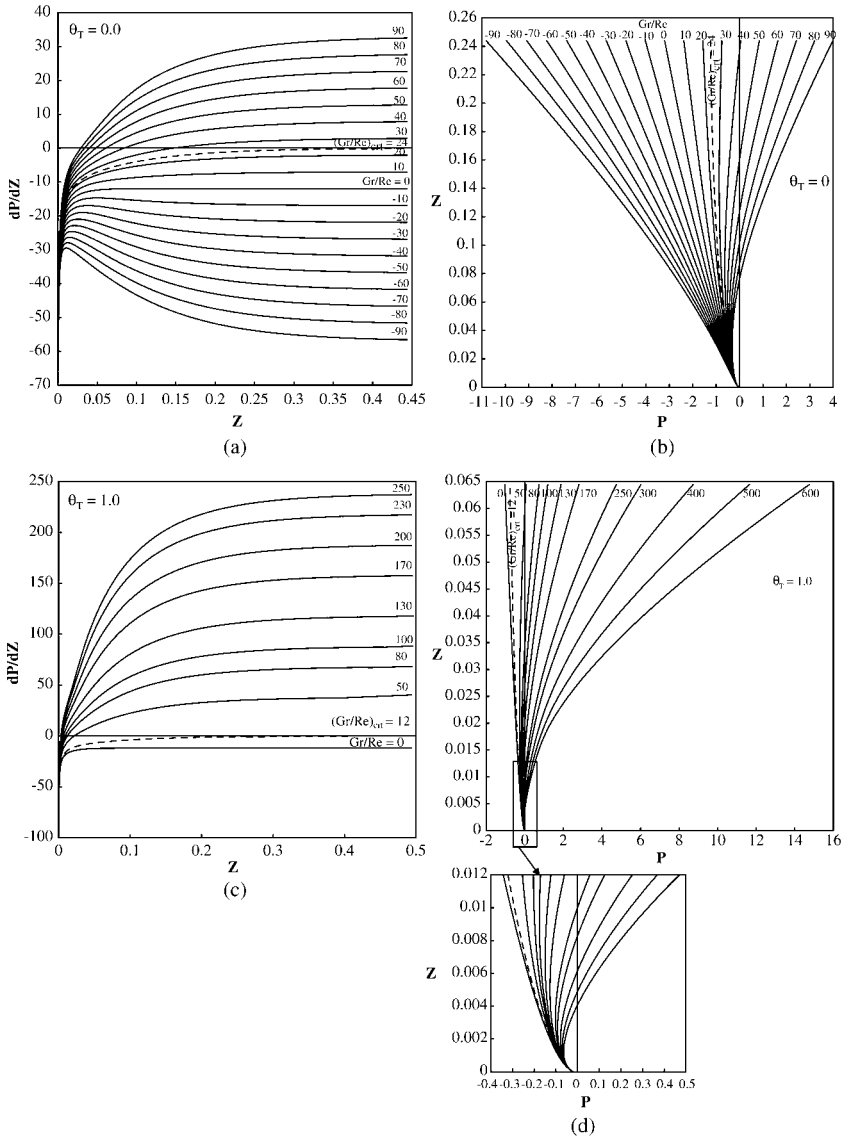

Notes: (a) Variation of pressure gradient; (b) pressure variation along the channel height for different Gr/Re for the thermal boundary condition of first kind and for $\theta_T = 0$; (c) variation of pressure gradient; (d) pressure variation along the channel height for different Gr/Re for the thermal boundary condition of first kind and for $\theta_T = 1$

Figure 7.

friction between the walls and the fluid which results in building up of two boundary layers over the two walls due to the viscous effects. These negative values of the pressure will continue increasing due to the corresponding negative pressure gradient for the cases of pure forced flow (Gr/Re = 0) and the buoyancy-opposed flow cases. For pure forced flow and buoyancy-opposed flows with low buoyancy effects, the pressure

gradient develops from a very high negative value at the entrance and continues negative with a decreasing negativity till it reaches asymptotically to its fully developed negative value. This behavior of the pressure gradient shows that both the viscous forces and buoyancy forces act in the same direction opposing the forced flow direction trying, both, to retard the flow. The direct result of the act of these two forces for buoyancy-opposed flow is to create and develop more negative pressure defect in the flow direction which is evidently presented in Figure 7(b). It is worth mentioning here that large values of the opposing buoyancy parameters lead to flow reversal and consequentially it leads faster to flow instability as shown in Table I.

On the other hand, for buoyancy-aided flow situations represented by the positive values of Gr/Re in Figures 7(a, b), the pressure defect develops from its zero value at the entrance acquiring negative value downstream due to the high negative pressure gradient at the entrance for all values of the buoyancy parameter Gr/Re. This negative pressure gradient with large negative values at the entrance develops downstream with a decreasing negativity approaching asymptotically its negative value for relatively low values of the buoyancy parameter Gr/Re. However, for large values of the buoyancy parameter Gr/Re for buoyancy-aided flow situations the pressure gradient develops from its very high negative value at the entrance with a decreasing negativity with an increasing rate such that it reaches zero and then continues increasing reaching asymptotically its fully developed positive value as shown in Figure 7(a). For situations of buoyancy-aided flow with relatively low values of the buoyancy parameter, Gr/Re, the buoyancy forces act in the same flow direction aiding the flow to overcome the viscous effects and the development of the pressure defect looks similar to that of pure forced flow but with lower negative values in the fully developed region (i.e. with less pressure drop along the channel). However, for buoyancy-aided flows with relatively large values of the buoyancy parameter, Gr/Re, the buoyancy forces aiding the flow develop downstream not only balancing out the viscous forces but also overcoming viscous forces resulting in pressure buildup. Within this positive range of the buoyancy parameter Gr/Re for buoyancy-aided flows, there exists a value of the buoyancy parameter at which the pressure gradient develops from the usual very high negative value at the entrance to its asymptotic value of exactly zero. This particular value of the Gr/Re, at which ($dP/dZ = 0$) exists only for buoyancy-aided flow as it is evidently shown in Figure 7(a). This particular value has been referred to as the critical value of Gr/Re, $(Gr/Re)_{crt}$. The existence of these critical values of Gr/Re has been mathematically demonstrated and its values were analytically obtained in section 3.1 above. The developments of the pressure gradient and the pressure defect for buoyancy-aided flow with the buoyancy parameter equals to $(Gr/Re)_{crt}$ are shown as dotted lines in Figures 7(a, b), respectively. For this particular case, the dimensionless pressure defect is developing from its zero value at the entrance acquiring a negative value due to the dominant viscous effects at this region. Further downstream, and due to the continuous heating, the buoyancy effects participate in controlling the flow and its effect develops in the flow direction till it balances exactly the viscous forces for this particular case resulting in exactly a zero pressure gradient in the fully developed region as shown in Figure 7(a) and consistently constant but negative pressure throughout the channel height till the fully developed conditions achieved as shown in Figure 7(b).

For buoyancy-aided flows with $Gr/Re > (Gr/Re)_{crt}$, the buoyancy forces acting in the flow direction are not effective directly after the channel entrance due to the time needed for the heat to penetrate and alter the fluid density resulting in a developing effect of the buoyancy forces which eventually overcome the viscous forces at distances

Table I.
Location of numerical instability, onset of flow reversal location and location of hydrodynamically fully development length in laminar mixed convection between vertical parallel plates for the thermal BC of first kind and for different θ_T

	$\theta_T = 0$			$\theta_T = 0.25$			$\theta_T = 0.5$			$\theta_T = 0.75$			$\theta_T = 1.0$	
Gr/Re	Z_{in}	Z_{fr}	Z_{fd}	Z_{in}	Z_{fr}	Z_{fd}	Z_{in}	Z_{fr}	Z_{fd}	Z_{in}	Z_{fr}	Z_{fd}	Z_{in}	Z_{fr}	Z_{fd}
0		NFR	0.06700		NFR	0.06700		NFR	0.06700		NFR	0.06700		NFR	0.06700
10		NFR	0.21430		NFR	0.22320		NFR	0.23246		NFR	0.24007		NFR	0.24591
20		NFR	0.28380		NFR	0.29380		NFR	0.30080		NFR	0.30480		NFR	0.30787
30		NFR	0.33780		NFR	0.34280		NFR	0.34480		NFR	0.34580		NFR	0.34380
40		NFR	0.38880		NFR	0.38480		NFR	0.37980		NFR	0.37480		NFR	0.36880
50		NFR	0.44280		NFR	0.42180		NFR	0.41080		NFR	0.39780		NFR	0.38880
60		NFR	0.51280		NFR	0.46280		NFR	0.43780		NFR	0.41980		NFR	0.40180
70		NFR	0.63680		NFR	0.50080		NFR	0.45980		NFR	0.43780		NFR	0.41480
80		0.20237	0.80980		NFR	0.55280		NFR	0.48780		NFR	0.45080		NFR	0.42780
90		0.12265	1.12380		NFR	0.60780		NFR	0.50780		NFR	0.46680		NFR	0.43680
100		0.09464	1.29080		NFR	0.89380		NFR	0.53780		NFR	0.48080		NFR	0.44280
150	0.20071	0.05322			0.09597	0.95980		NFR	0.73380		NFR	0.53887		NFR	0.47680
200	0.06103	0.04091		0.11570	0.06674			0.16340	0.85480		NFR	0.59380		NFR	0.48480
230	0.06072	0.03669		0.09075	0.05832			0.13050			NFR	0.62380		NFR	0.50180
250	0.04899	0.03453		0.08140	0.05432			0.11670			NFR	0.63880		NFR	0.50680
300	0.04340	0.03067		0.06288	0.04698		0.32380	0.09420			0.69980	0.94080		NFR	0.51080
400	0.04047	0.02578		0.05716	0.03813		0.09550	0.07110			0.22140			NFR	0.55380
500	0.03283	0.02288		0.04047	0.03301		0.07010	0.05981		7.50950	0.17490			NFR	0.55980
600	0.02798	0.02075		0.03569	0.02847		0.06640	0.05107		0.34080	0.15130			NFR	0.57387
700	0.02702	0.01926		0.03395	0.02503		0.03669	0.03015		0.18860	0.13390			NFR	0.58780

Note: NFR – no flow reversal

that depend on the value of Gr/Re (heating rates). These distances are nothing but the distance from the entrance to the locations at which the developing negative pressure gradient crosses the line of zero value and inverts its sign to be a positive pressure gradient. For such situations, the dimensionless pressure defect will also develop from its zero value at the entrance acquiring negative value due to the friction at the entrance. This is a direct result of the viscous effects at the entrance, which will be gradually balanced and eventually overcome by the developing buoyancy forces. This results in a buildup of the pressure making the pressure defect develop gradually with a decreasing negativity till it crosses the line of zero pressure defect and continue building up creating a monotonically increasing positive pressure as shown in Figure 7(b). On the other hand for values of $(Gr/Re) < (Gr/Re)_{crt}$,, both the pressure gradient and the pressure defect acquire negative values throughout the downstream of the channel entrance. Similar results but for the case of $\theta_T = 1$ are shown in Figures 7(c) and (d), respectively.

These four Figures 7(a-d) are only sample of the results obtained from the investigated cases. It is clear from these four figures that for situations with $(Gr/Re) > 0$, the buoyancy effects act in the flow direction aiding the flow, to overcome the friction due to the fluid viscous effects. This would definitely results in reducing the load on the pumping device (pump for liquid and compressor for gases). For buoyancy-aided flows with $(Gr/Re) > (Gr/Re)_{crt}$ the pressure buildup due to the buoyancy effects explained earlier results in monotonically increasing positive pressure. For relatively higher values of $(Gr/Re) \gg (Gr/Re)_{crt}$, the channel would have higher buoyancy forces that make the channel, due to high heating rates, act as a diffuser and the pumping device in such cases might work as a flow regulator (this was noticed and reported by Han, 1993). However, for very high heating rates the pressure buildup, due to the buoyancy-aiding effects, might result in a back pressure that is high enough to prevent the fluid particles to continue flowing downstream the vertical channel in a similar fashion to boundary layer separation in external flow over surfaces. In such situations, flow reversal takes place, especially near the cold wall (for cases of asymmetric heating) where the buoyancy effects are weaker. The locations of the flow reversal onset in such situation was defined as the locations at which the velocity gradient at the wall ($(\partial U/\partial Y) \leq 0$). These locations (if any) are reported in Table I. Increasing more the heating rate (Gr/Re) makes the flow reversal become more severe and the flow will suffer from flow instability, which directly leads to numerical instability and the computer code stops, since it is not formulated to solve flow instability problems. The locations of the flow/numerical instability are indicated also in Table I. It is worth noting here that the case of symmetric heating ($\theta_T = 1.0$) with buoyancy-aided flow never suffers from flow reversal. This is attributed to the fact that for buoyancy-aided flow situations, the buoyancy effects develop faster near both of the heated walls, in this particular case, helping the flow to overcome the viscous effects. This is not the case of asymmetric heating, especially when there is a big difference of temperature of the two walls of the channel. Figures 8(a, b) depict graphical presentations of the developing velocity profiles along a vertical channel between two parallel plates under buoyancy-aided flow situations with asymmetric and symmetric heating conditions, particularly with $\theta_T = 0$ and $\theta_T = 1.0$, respectively. It is clear from these two figures that flow reversal will take place near the cold wall for the case of asymmetric heating, $\theta_T = 0$, where the buoyancy forces are weaker than overcoming the back pressure developed far downstream the channel. On the other hand, flow reversal will never take place in the case of symmetric heating, $\theta_T = 1.0$ due to the buoyancy effects that are

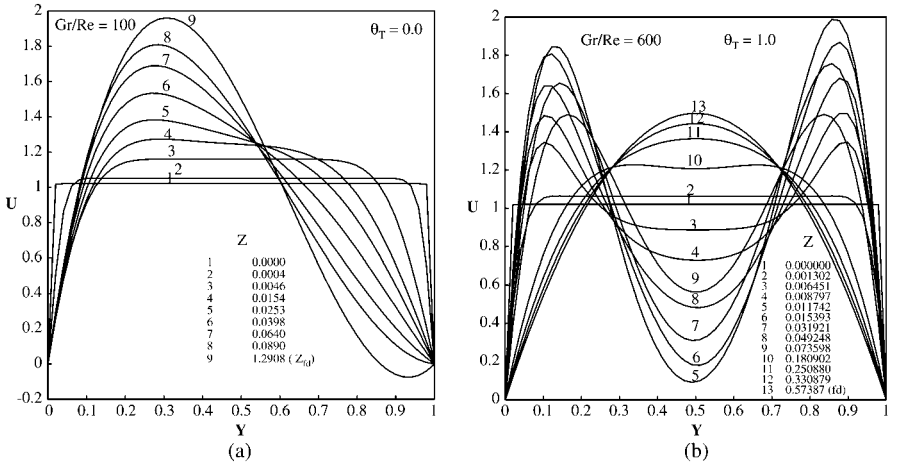

Figure 8.
Development of the velocity profiles along the channel

Notes: (a) $\theta_T = 0$; (b) $\theta_T = 1.0$

strong enough, near the two heated walls, to overcome the back pressure buildup, within the investigated range of the buoyancy parameter, Gr/Re.

There are two important hydrodynamic parameters. The first one is the location at which the pressure gradient, for buoyancy-aided flow with the buoyancy parameter $(Gr/Re) > (Gr/Re)_{crt}$, crosses the line of zero value changing its sign from negative pressure gradient to positive pressure gradient (Z_I). This represents the location at which pressure buildup started. This pressure buildup results in increasing the pressure defect from the negative value downstream the entrance with a positive pressure gradient such that it reaches zero at location (Z_{II}), the second important hydrodynamic parameter, where it increases monotonically and positively downstream. This location, Z_{II}, is obtained for all the investigated cases and is reported in Table II. The location, Z_{II}, represents the height beyond which a vertical channel with buoyancy-aided flow condition can act as a diffuser under a given isothermal boundary condition. Caution should be taken in determining the operating heating rates represented in terms of the buoyancy parameter Gr/Re such that flow reversal due to pressure buildup can be avoided. The information that is obtained and presented, in Table II, for different isothermal boundary conditions for different values of Gr/Re would be of prime importance to the designer of heat transfer and flow equipment. Such information would definitely help the designer to properly size the pump or compressor needed to pump the fluid through channels subjected to buoyancy-aided flow situations. It is clear that making the design and sizing of the pump based on pure forced flow conditions would result in an oversized pumping device, if the flow is buoyancy-aided flow or undersized if the flow is buoyancy-opposed flow. The development of the pressure gradient and the pressure defect along a vertical channel between parallel plates under thermal boundary condition of first kind have been plotted in Figures 9(a, b) for a given value of the buoyancy parameter $(Gr/Re) = 50$ at different values of θ_T. These two figures show that the effect of the buoyancy forces, on the development of the pressure gradient and the pressure, increases with the increase of the temperature ratio of the cold wall with respect to that of the hot wall, θ_T. This is clearly attributed to the increase of heating rates that increases with the increase of the temperature ratio of the cold wall till its temperature

Gr/Re	$\theta_T = 0$		$\theta_T = 0.25$		$\theta_T = 0.5$		$\theta_T = 0.75$		$\theta_T = 1.0$	
	Z_I	Z_{II}	Z_I	Z_{II}	Z_I	Z_{II}	Z_I	Z_{II}	Z_I	Z_{II}
20			0.28771	[a]	0.13907	[a]	0.09791	[a]	0.07607	0.23046
30	0.13465	0.51268	0.08433	0.26193	0.06176	0.18209	0.04844	0.14082	0.03958	0.11513
40	0.07402	0.22356	0.05210	0.15056	0.03948	0.11435	0.03141	0.09224	0.02587	0.07726
50	0.05219	0.14827	0.03727	0.10707	0.02834	0.08370	0.02265	0.06855	0.01874	0.05797
60	0.04009	0.11224	0.02846	0.08338	0.02169	0.06595	0.01741	0.05439	0.01448	0.04623
70	0.03205	0.09083	0.02263	0.06829	0.01735	0.05430	0.01401	0.04496	0.01170	0.03836
80	0.02621	0.07651	0.01856	0.05776	0.01434	0.04605	0.01163	0.03825	0.00973	0.03275
90	0.02187	0.06615	0.01563	0.04995	0.01215	0.03991	0.00989	0.03326	0.00829	0.02856
100	0.01858	0.05824	0.01342	0.04393	0.01050	0.03517	0.00857	0.02940	0.00718	0.02532
130	0.01252	0.04252	0.00929	0.03202	0.00732	0.02587	0.00598	0.02181	0.00499	0.01889
150	0.01018	0.03574	0.00762	0.02703	0.00601	0.02197	0.00488	0.01861	0.00400	0.01616
200	0.00679	0.02507	0.00508	0.01937	0.00391	0.01595	0.00292	0.01360	0.00122	0.01186
250	0.00493	0.01912	0.00355	0.01506	0.00138	0.01250	0.00100	0.01070	0.00087	0.00934
300	0.00365	0.01542	0.00122	0.01230	0.00093	0.01026	0.00081	0.00880	0.00073	0.00769
400	0.00098	0.01109	0.00080	0.00897	0.00071	0.00752	0.00064	0.00646	0.00059	0.00566
500	0.00077	0.00863	0.00066	0.00703	0.00059	0.00591	0.00054	0.00508	0.00050	0.00445
600	0.00066	0.00704	0.00058	0.00576	0.00052	0.00485	0.00048	0.00418	0.00044	0.00366
700	0.00059	0.00592	0.00052	0.00486	0.00047	0.00410	0.00043	0.00353	0.00040	0.00309

Note: [a]For such cases, the pressure defect did not cross the value of zero before the fully developed conditions

Table II.
Location of zero pressure gradient and location onset of pressure build up between vertical parallel plates for the thermal BC of first kind and for different θ_T

reaches that of the hot wall. These increasing buoyancy forces with the increase of θ_T engender more induced flow through the channel which helps the flow to overcome faster the viscous forces near the two walls. This results in changing the pressure gradient its sign from negative to positive at a location closer to the channel entrance. Consequently, pressure buildup commences also closer to the channel entrance for higher values of θ_T. In other words, Z_I and Z_{II} become closer to the channel entrance with the increase of θ_T as it is evidently clear from Figures 9(a, b) and Table III. Due to its importance, the values of Z_I and Z_{II} under thermal boundary conditions of the first kind are plotted as function of the buoyancy parameter Gr/Re for different values of θ_T in Figures 9 (c) and (d), respectively.

Effect of Prandtl number on the hydrodynamic parameters for laminar mixed convection in vertical channel between parallel plates has been studied by closely investigating the behavior of pressure gradient and pressure defect in the developing region for fluids of different Prandtl number. The results were plotted for slightly below and above critical value of buoyancy parameter $(Gr/Re)_{crt}$ for fluid of $Pr = 1$, 10 and 100 under the isothermal boundary condition with $\theta_T = 0$. These values of Prandtl number were selected to cover a considerable range of the fluids that are in common practical and industrial use. A Prandtl number of order 1 represents gaseous fluids with the particular value of 0.7 for air. The Prandtl number of order 10 represents liquids such as water while Prandtl number of order 100 represents viscous oils. Unpresented figures show the variation of pressure gradient and pressure defect as a function of axial distance for different values of buoyancy parameter Gr/Re for each of the investigated Prandtl numbers. All the figures exhibit similar behavior as that presented for all cases of $Pr = 0.7$. It is worth mentioning here that Prandtl number has no effect on the critical value of $(Gr/Re)_{crt}$ under hydrodynamically and thermally fully developed conditions. This can be easily shown analytically and it was confirmed

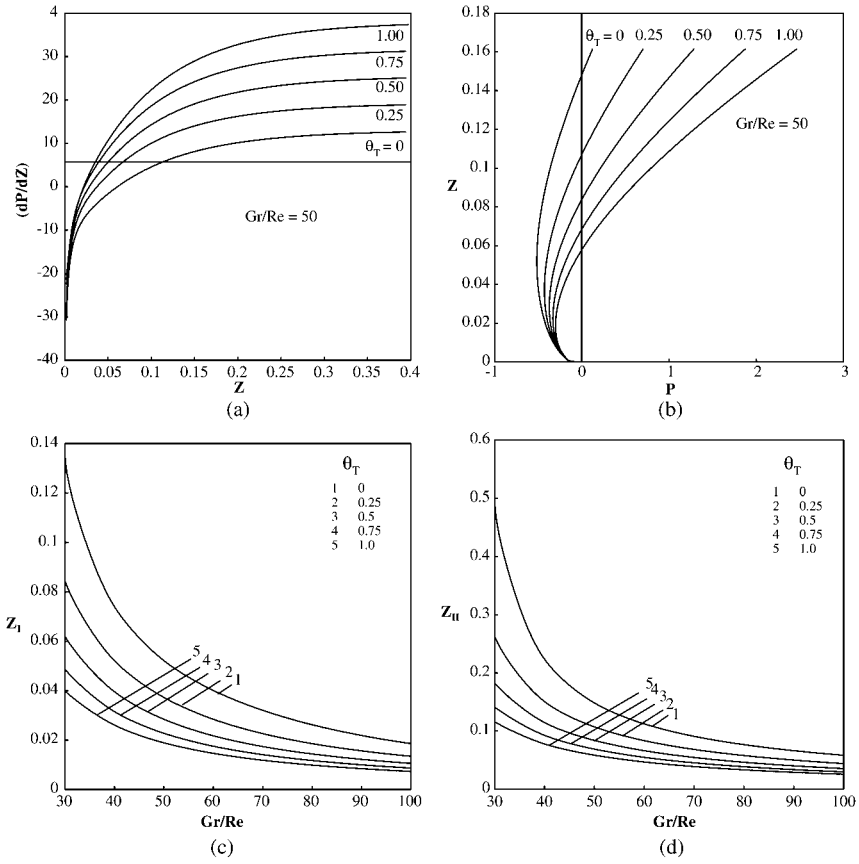

Notes: (a) Development of the pressure gradient; (b) development of the pressure for different θ_T at (Gr/Re) = 50 and graphical presentation of locations of: (c) zero pressure gradient; (d) zero dimensionless pressure, as a function of Gr/Re for different θ_T

Figure 9.

Pr	Z_I	(Gr/Re) = 30 > $(Gr/Re)_{crt}$, $\theta_T = 0$ Z_{II}	Z_{fd}
0.7	0.1347	0.5127	0.3378
1	0.2087	0.7155	0.9238
10	2.0584	6.2967	8.3806
100	20.2054	62.0514	71.4482

Table III.
Effect of Prandtl number on Z_I and Z_{II} and Zfd

numerically through the present investigation. The pressure gradient vanished for all the investigated Prandtl numbers when the critical values that was obtained analytically for the buoyancy parameters $(Gr/Re)_{crt}$ was used as input to the numerical code. However, the locations at which the developing pressure gradient crosses the zero value which are the locations of positive pressure gradient incipient, Z_I, and the locations of pressure buildup onset, Z_{II}, for (Gr/Re) > $(Gr/Re)_{crt}$ as well as the fully

developed length vary with the variation of the Prandtl number. Table III gives an example of the variation of the above-mentioned locations with Prandtl number for isothermal boundary condition with $\theta_T = 0$.

7. Pressure drop reduction and heat transfer enhancements

The numerical results of the pressure development for different values of θ_T (e.g. those presented in Figures 7(b) and 6(d) for $\theta_T = 0$ and $\theta_T = 1$, respectively) for buoyancy-aided and buoyancy-opposed flows indicated clearly that for buoyancy-opposed flows, the increase of the buoyancy parameter increases the pressure drop along a given length of the channel. On the other hand, for buoyancy-aide flows, the increase of the buoyancy parameter decreases the pressure drop along a given length of the channel for all values of the buoyancy parameter in the range $0 < (Gr/Re) < (Gr/Re)_{crt}$. Moreover, for buoyancy-aided flows with $(Gr/Re) > (Gr/Re)_{crt}$, pressure build up might take place if the channel is high enough with a possible incipient of flow reversal. It is worth repeating here that these trends of the pressure development for different values of the buoyancy parameter were reported by Aung and Worku (1986b) as presented in Figure 6(b).

On the other hand, the numerical results of the developing flow under mixed convection through vertical channels between parallel plates under isothermal boundary conditions revealed clearly that the increase of the buoyancy parameter enhances the heat transfer. In this regard, the development of the Nusselt number on the heat transfer wall and the opposite wall of the channel has been numerically estimated. To estimate the Nusselt number at the two walls of the channel, the developing temperature profiles along with the developing velocity profiles, are used to obtain the development of the mean bulk fluid temperature as described by Equation (25):

$$\theta_m = \frac{\int_0^1 \theta(Y)\, U(Y)\, dY}{\int_0^1 U(Y)\, dY} \tag{25}$$

Equation (25) is evaluated numerically. The developing mean bulk fluid temperature is used to obtain the developing Nusselt number at the active and passive plates of the channel as described by Equations (28a) and (28b), respectively.

$$Nu_1 = \frac{-2}{(1-\theta_m)} \left.\frac{d\theta}{dY}\right|_{Y=0} \tag{26a}$$

$$Nu_2 = \frac{2}{(\theta_T-\theta_m)} \left.\frac{d\theta}{dY}\right|_{Y=1} \tag{26b}$$

It is worth mentioning that the factor of 2 is introduced in Equations (26a) and (26b) to make Nusselt number consistent with that reported in the literature (Shah and London, 1978). This is to count for the difference in the definition of the characteristic length used in the present study as the channel width that is defined presently as while it is defined as *2b* in Shah and London (1978).

The development of the Nusselt number on the heat transfer wall and the opposite wall of the channel are shown in Figures 10(a) and (b) for the case of $\theta_T = 0$. These two figures show that the Nusselt number on the heat transfer increases with the increase

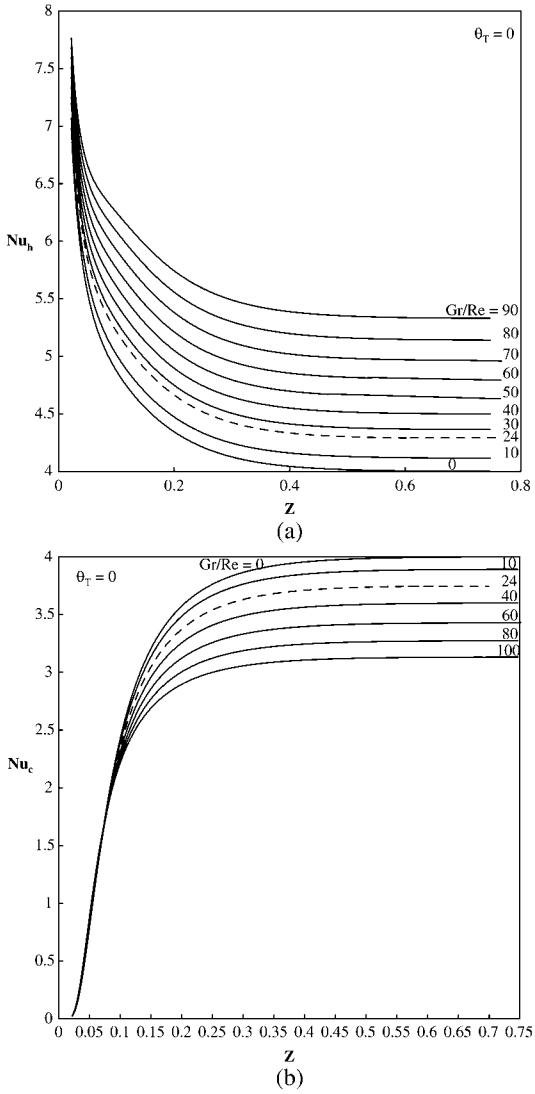

Notes: (a) Variation of Nusselt number on the heated side of the channel vs axial distance for different Gr/Re for the thermal BC of first kind and for $\theta_T = 0$ between vertical parallel plates; (b) variation of Nusselt number on the cold side of the vertical channel versus axial distance (Z) for different Gr/Re for the thermal BC of first kind and for $\theta_T = 0$ between vertical parallel plates

Figure 10.

of the buoyancy parameter while that on the opposite wall decreases with the buoyancy parameter. This increase/decrease of the Nusselt number on the active/opposite wall, results in an increase in the heat absorbed by the fluid flow in through the channel. The heat absorbed by the fluid is represented by the development of the mean bulk fluid temperature as shown in Figure 11 for different values of the buoyancy

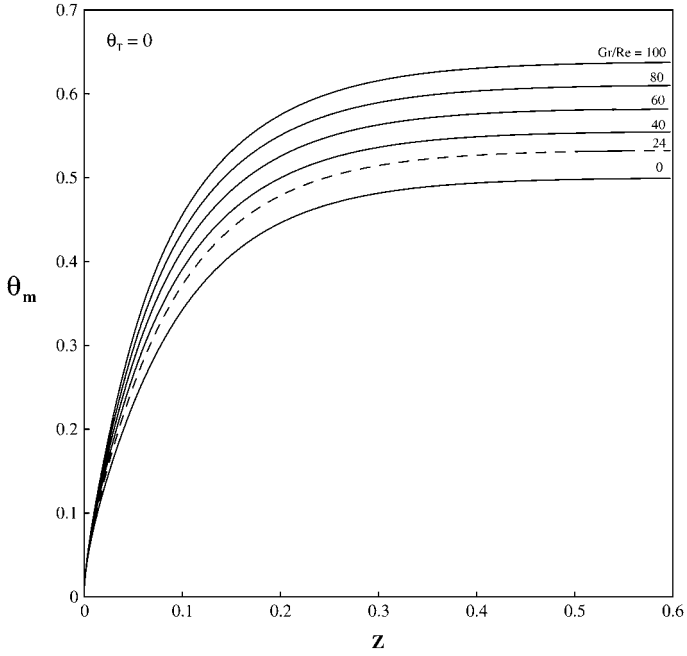

Figure 11.
Mean or bulk temperature along the channel height for different Gr/Re for the thermal boundary condition of first kind and for $\theta_T = 0$ between vertical parallel plates

parameter for buoyancy-aided flow with $\theta_T = 0$. One of the important parameters in heat transfer equipment is the amount of heat transfer per unit of the pumping power. The net rate of heat transfer in the present calculation is to be taken as the heat absorbed by the fluid from the entrance to a given section in the channel. On the other hand, the pumping power will be taken as the usual as the product of the flow rate and the pressure drop from the entrance to the given section of the channel. Figure 12 shows the effect of the buoyancy parameter on the ratio of the heat transfer to the pumping power for buoyancy-aided flow situations. This figure shows clearly that the heat transfer per unit of the pumping power is significantly enhanced due to the increase of the buoyancy parameter for buoyancy-aided flow for buoyancy parameter below that causes pressure build up and the consequent flow reversal.

8. Conclusions

Buoyancy effects on the fully developed and developing hydrodynamic parameters such as pressure and pressure gradient in the flow direction for a forced flow through vertical channels between parallel plates have been numerically investigated under the thermal boundary conditions of first kind. The investigation covers a wide range of the buoyancy parameters Gr/Re for buoyancy-opposed and buoyancy-aided flow situations. The analytical solution of the fully developed governing equations revealed the presence of critical values of the buoyancy parameter $(Gr/Re)_{crt}$ at which the buoyancy forces balance out the viscous forces. On the other hand, the numerically obtained results confirmed the presence of these conditions. At these conditions, the pressure gradient develops from its usual high negative value at the entrance with a decrease in its negativity till it reaches asymptotically its exact value of zero. Buoyancy parameters greater than these critical values result in building-up the pressure downstream the entrance such that the vertical channel might act as a thermal diffuser with possible incipient of flow reversal. Locations

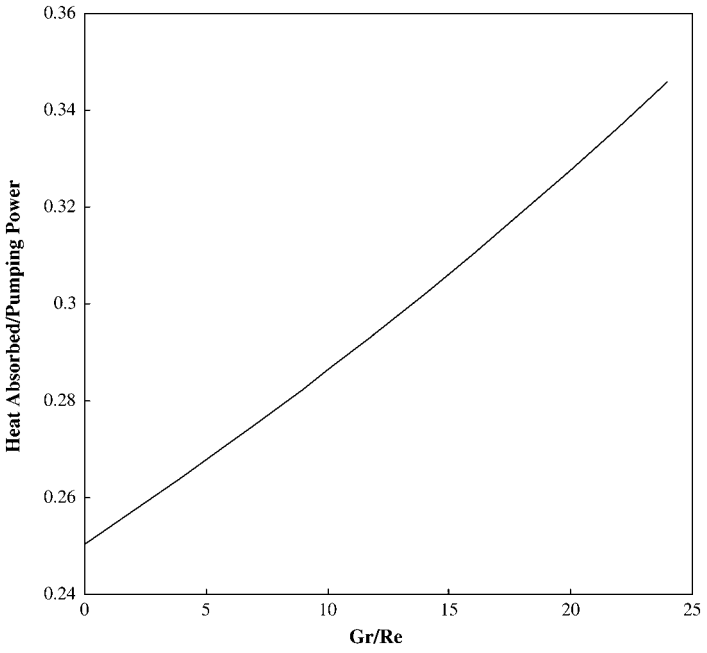

Figure 12.
Variation of the heat absorbed per unit of the pumping power with buoyancy parameter Gr/Re for the thermal boundary condition of first kind and for $\theta_T = 0$ between vertical parallel plates

at which the pressure gradient vanishes and the locations at which the pressure-buildup starts have been numerically obtained and presented for all the investigated cases. Conditions for flow reversal have been obtained analytically for buoyancy-opposed and buoyancy-aided flows as (Gr/Re) $\geq$ 72/ (1$-$ θ_T). Flow reversal in buoyancy-aided flow situations is attributed to the high pressure build up due to higher buoyancy effects corresponding to higher heating rates. This high pressure build up prevents the relatively slow particles near the wall from penetrating more down stream in a similar fashion to boundary layer separation in external flow over surfaces. Locations of flow reversal onset for buoyancy-aided flows or the locations at which buoyancy-aided flow is converted to buoyancy-opposed flow and the consequent higher pressure buildup in the flow direction as well as the locations of flow instability due to flow reversal have been also calculated and presented for all the investigated cases. These locations become closer to the entrance with increase of Gr/Re. Numerical values of the hydrodynamic development length which increases due to higher heat transfer rates represented by higher values of Gr/Re are presented. Effects of Prandtl number on some of the above-mentioned parameters have been investigated and presented for one of the investigated thermal boundary conditions as an example. The results clearly show that for buoyancy-aided flow, the increase of the buoyancy parameter enhances the heat transfer and reduces the pressure drop across the vertical channel.

References

Aung, W. and Worku, G. (1986a), "Theory of fully developed combined convection including flow reversal", *Transactions of the ASME, Journal of Heat Transfer*, Vol. 108, pp. 485-8.

Aung, W. and Worku, G. (1986b), "Developing flow and flow reversal in a vertical channel with asymmetric wall temperatures", *Transactions of the ASME, Journal of Heat Transfer*, Vol. 108, pp. 299-307.

Aung, W. (1987), "Mixed convection in internal flow", in Kakaç, S., Shah, R.K. and Aung, W. (Eds), *Hand Book of Single-Phase Convective Heat Transfer*, Chapter 15, John Wiley & Sons, New York, NY.

Barletta, A. (2001), "Analysis of flow reversal for laminar mixed convection in a vertical rectangular duct with one or more isothermal walls", *International Journal of Heat and Mass Transfer*, Vol. 44 No. 18, pp. 3481-297.

Barletta, A. and Zanchini, E. (1999), "On the choice of reference temperature for fully developed mixed convection in a vertical channel", *International Journal of Heat and Mass Transfer*, Vol. 42 No. 16, pp. 3169-81.

Barletta, A., Nobile, E., Pinto, F., Rossi di Schio, E. and Zanchini, E. (2006), "Natural convection in a 2D-cavity with vertical isothermal walls: cross-validation of two numerical solutions", *International Journal of Thermal Sciences*, Vol. 45, pp. 917-22.

Behazadmher, A., Galanis, N. and Laneville, A. (2003), "Low Reynolds number mixed convection in vertical tubes with uniform wall heat flux", *International Journal of Heat and Mass Transfer*, Vol. 46, pp. 4823-33.

Boulama, K. and Galanis, N. (2004), "Analytical solution for fully developed mixed convection between parallel vertical plates with heat and mass transfer", *Transactions of ASME, Journal of Heat Transfer*, Vol. 126, pp. 381-8.

Cebeci, T, Khattab, A.A. and LaMont, R. (1982), "Combined natural and forced convection in vertical ducts. Heat transfer", *Proceedings of the 7th International Heat Transfer Conference*, *Munich*, Vol. 3, pp. 419-24.

Cimpean, D., Pop, I., Ingham, D.P. and Merkin, J.H. (2009), "Fully developed mixed convection flow between inclined parallel plates filled with a porous medium", *Transport in Porous Media*, Vol. 77 No. 1, pp. 87-102.

Du, S-Q., Bilgen, E. and Vasseur, P. (1998), "Mixed convection heat transfer in open ended channels with protruding heaters", *Heat and Mass Transfer*, Vol. 34 No. 4, pp. 263-70.

El-Shaarawi, M.A.I. and Sarhan, A. (1980), "Free convection effects on the developing laminar flow in vertical concentric annuli", *ASME Journal of Heat Transfer*, Vol. 102, pp. 617-22.

Gau, C., Yih, K.A. and Aung, W. (1992), "Reversed flow structure and heat transfer measurements for buoyancy-assisted convection in a heated vertical duct", *ASME Journal of Heat Transfer*, Vol. 114, pp. 928-35.

Hamadah, T.T. and Wirtz, R.A. (1991), "Analysis of laminar fully developed mixed convection in a vertical channel with opposing buoyancy", *Transactions of ASME, Journal of Heat Transfer*, Vol. 113, pp. 507-10.

Hammou, Z.A., Benhamou, B., Galanis, N. and Orfi, J. (2004), "Laminar mixed convection of humid air in a vertical channel with evaporation or condensation at the wall", *International Journal of Thermal Sciences*, Vol. 43, pp. 531-9.

Han, J.C. (1993), "Hydraulic characteristics of mixed convection in a heated vertical pipe", *Transactions of the ASME, Journal of Fluid Engineering*, Vol. 115, pp. 41-7.

Huang, T.M., Gau, C. and Aung, W. (1995), "Mixed convection flow and heat transfer in a heated vertical convergent channel", *International Journal of Heat and Mass Transfer*, Vol. 38 No. 13, pp. 2445-56.

Inagaki, T. and Komori, K. (1995), "Numerical modeling on turbulent transport with combined forced and natural convection between two vertical parallel plates", *Numerical Heat Transfer, Part A*, Vol. 27 No. 4, pp. 417-31.

Ingham, D.B., Keen, D.J. and Heggs, P.J. (1988), "Flows in vertical channels with asymmetric wall temperatures and including situations where reverse flows occur", *Transactions of ASME, Journal of Heat Transfer*, Vol. 110, pp. 910-17.

Kasagi, N. and Nishimura, M. (1997), "Direct numerical simulation of combined forced and natural turbulent convection in a vertical plane channel", *International Journal of Heat and Fluid Flow*, Vol. 18 No. 1, pp. 88-99.

Mete, A. and Orhan, A. (2007), "Mixed convection in a vertical parallel plate microchannel with asymmetric wall heat fluxes", *ASME Journal of Heat Transfer*, Vol. 129 No. 8 (Technical Briefs, p. 1091 (5pp.)).

Miyatake, O. and Fujii, T. (1972), "Free convection heat transfer between vertical parallel plates-one is isothermally heated and the other is thermally insulated", *KAGAKU KOGAKU, Society of Chemical Engineers, Japan*, Vol. 36, pp. 405-12.

Mokheimer, E.M.A. and El-Shaarawi, M.A.I. (2004a), "Developing mixed convection in vertical eccentric annuli", *Heat and Mass Transfer*, Vol. 41 No. 2, pp. 176-87.

Mokheimer, E.M.A. and El-Shaarawi, M.A.I. (2004b), "Critical values of Gr/Re for mixed convection in vertical eccentric annuli with isothermal/adiabatic walls", *ASME Journal of Heat Transfer*, Vol. 126, pp. 479-82.

Mokheimer, E.M.A. and Sami, S. (2006), "Conditions for pressure build-up due to buoyancy effects on forced convection in vertical eccentric annuli under thermal boundary condition of first kind", *Heat and Mass Transfer*, Vol. 43 No. 2, pp. 175-89.

Sami, S. (2005), "Laminar mixed convection in vertical channels", MSc thesis, King Fahd University for Petroleum and Minerals, Dhahran.

Shah, R.K. and London, A.L. (1978), "Laminar flow forced convection in ducts", *Advances in Heat Transfer*, Vol. 1, Supplement 1, 450 pp.

Szpiro, O., Lewis, J.S. and Collins, M.W. (1984), "Numerical solutions for developing combined convection between uniformly heated vertical parallel plates", *Institution of Chemical Engineers Symposium Series*, Vol. 86, pp. 829-38.

Wirtz, R.A. and McKinley, P. (1985), "Buoyancy effects on downward laminar convection between parallel plates", *ASME, Heat Transfer Division, (Publication) HTD*, Vol. 42, pp. 105-12.

Yao, L.S. (1983), "Free and forced convection in the entry region of a heated vertical channel", *International Journal of Heat and Mass Transfer*, Vol. 26 No. 1, pp. 65-72.

Corresponding author
B.S. Yilbas can be contacted at: bsyilbas@kfupm.edu.sa